Autophagy is required for the rejection of self-incompatible pollen in two accessions of transgenic *Arabidopsis thaliana*

Stuart R. Macgregor,[a] Hyun Kyung Lee,[a,1] Hayley Nelles,[a] Daniel C. Johnson,[a] Tong Zhang,[b] Chaozhi Ma,[b] and Daphne R. Goring[a,c,2,3]

[a]Department of Cell & Systems Biology, University of Toronto, Toronto, Canada M5S 3B2.
[b]National Key Laboratory of Crop Genetic Improvement, National Center of Rapeseed Improvement in Wuhan, Huazhong Agricultural University, Wuhan 430070, China.
[c]Centre for the Analysis of Genome Evolution & Function, University of Toronto, Toronto, Canada M5S 3B2.

[1]Current address: Dept. Plant Molecular Biology, University of Lausanne, Switzerland.

[2]Author for Contact, [3]Senior author: Daphne Goring d.goring@utoronto.ca

Short Title: Autophagy in *Arabidopsis* self-incompatibility

One Sentence Summary: In self-incompatible transgenic *Arabidopsis thaliana* lines, autophagy is an integral part of the cellular responses in the stigma to efficiently block fertilization by self-incompatible pollen.

Author Contributions: DRG conceived the project; DRG, SRM, HKL, HN, DCJ and TZ conceptualized and designed experiments; SRM performed crosses, generated and analyzed data for the SI-C24 *atg7-9* plants, SI-Col-0 *atg5-1* plants, and the SI-Col-0 *atg7-2* GFP-ATG8a imaging; HKL and SRM performed crosses, generated and analyzed data for the SI-Col-0 *atg7-2* plants; HN and DCJ performed preliminary work on the SI lines and imaging; TZ generated the SI-Col-0 line; DRG and CM supervised the experiments; SRM, HKL, and DRG wrote the manuscript; All authors commented on the manuscript before submission; DRG agrees to serve as the author responsible for contact and ensures communication.

Funding information: This research was supported by a grant from Natural Sciences and Engineering Research Council of Canada to DRG, SRM was supported by the Rustom H. Dastur Graduate Scholarship, and HKL was supported by an Ontario Graduate Scholarship.

Abstract

Successful reproduction in the Brassicaceae is mediated by a complex series of interactions between the pollen and the pistil, and some species have an additional layer of regulation with the self-incompatibility trait. While the initial activation of the self-incompatibility pathway by the pollen S-locus protein11/*S*-locus cysteine-rich peptide and the stigma *S* Receptor Kinase is well characterized, the downstream mechanisms causing self-pollen rejection are still not fully understood. In previous studies, we had detected the presence of autophagic bodies with self-incompatible pollinations in *Arabidopsis lyrata* and transgenic *A. thaliana* lines, but it was not known if autophagy was essential for self-pollen rejection. Here, we investigated the requirement of autophagy in this response by crossing mutations in the essential *AUTOPHAGY7* (*ATG7*) or *AUTOPHAGY5* (*ATG5*) genes into two different transgenic self-incompatible *A. thaliana* lines in the Col-0 and C24 accessions. By using these previously characterized transgenic lines that express *A. lyrata* and *A. halleri* self-incompatibility genes, we demonstrated that disrupting autophagy can weaken their self-incompatible responses in the stigma. When the *atg7* or *atg5* mutations were present, an increased number of self-incompatible pollen were found to hydrate and form pollen tubes that successfully fertilized the self-incompatible pistils. Additionally, we confirmed the presence of GFP-ATG8a labelled autophagosomes in the stigmatic papillae following self-incompatible pollinations. Together, these findings support the requirement of autophagy in the self-incompatibility response and add to the growing understanding of the cellular events that take place in the stigma to reject self-pollen.

Key words

Autophagy, self-incompatibility, pollen-pistil interactions, reproduction, *SP11/SCR*, *SRK*, *ARC1*, *ATG7, ATG5, GFP-ATG8a*

62 **Introduction**

63 Reproduction in the Brassicaceae is a tightly controlled process, with many components
64 contributing to successful pollen-pistil interactions (reviewed in Doucet et al., 2016; Mizuta and
65 Higashiyama, 2018; Johnson et al., 2019; Adhikari et al., 2020). The Brassicaceae dry stigma
66 lacks surface secretions and instead regulates the delivery of resources to the pollen shortly after
67 pollination. This leads to the selective hydration of compatible pollen grains, followed by the
68 penetration of the pollen tube into the stigmatic barrier to grow down the reproductive tract
69 (reviewed in Dickinson, 1995; Palanivelu and Tsukamoto, 2012; Doucet et al., 2016; Adhikari et
70 al., 2020). It is also at this initial cell-cell communication stage that self-incompatible pollen is
71 recognized and blocked by the stigma to prevent inbreeding (reviewed in Jany et al., 2019;
72 Nasrallah, 2019; Durand et al., 2020). A recent live-cell imaging study in *Arabidopsis thaliana*
73 compared pollen hydration rates of compatible and self-incompatible pollen grains and found
74 that while compatible pollen grains rapidly hydrated, self-incompatible pollen failed to fully
75 hydrate which then led to a failure in pollen germination or a failure of pollen tubes to penetrate
76 the stigmatic papilla cell wall (Rozier et al., 2020). Furthermore, actin foci were present in the
77 stigmatic papillae at the site of emerging pollen tubes for compatible pollen only. The actin
78 focalization is likely associated with the stigmatic papilla cellular responses to enable compatible
79 pollen hydration and pollen tube penetration (Rozier et al., 2020).

80 The Brassicaceae self-incompatible response is initiated by the binding of the *S*-haplotype-
81 specific pollen ligand, *S*-locus protein 11/*S*-locus cysteine-rich peptide (SP11/SCR) to the
82 corresponding stigma-specific *S* Receptor Kinase (SRK). This leads to the phosphorylation of the
83 SRK kinase domain and activation of the downstream signaling responses, ultimately leading to
84 the rejection of the self-incompatible pollen grain reviewed in Jany et al., 2019; Nasrallah, 2019).
85 Not all Brassicaceae species possess this trait due to mutations in the key self-incompatibility
86 genes, *SP11/SCR* and *SRK* (reviewed in Durand et al., 2020). For example, the transition of *A.*
87 *thaliana* to a fully selfing species is associated with mutations in the *SCR* and *SRK* genes
88 (Kusaba et al., 2001; Shimizu et al., 2008; Boggs et al., 2009; Tsuchimatsu et al., 2010; Guo et
89 al., 2011; Tsuchimatsu et al., 2017). In contrast, other family members like *A. lyrata* and *A.*
90 *halleri* have intact *SCR* and *SRK* genes, which result in a robust self-incompatibility response
91 upon self-pollination (Kusaba et al., 2001; Schierup et al., 2001; Goubet et al., 2012).

92 A number of studies have reintroduced the self-incompatibility trait back into *A. thaliana* by
93 introducing *A. lyrata* or *A. halleri SP11/SCR* and *SRK* transgenes (Nasrallah et al., 2004; Boggs
94 et al., 2009; Indriolo et al., 2014; Iwano et al., 2015; Zhang et al., 2019; Rozier et al., 2020).
95 However, the success of this approach was accession-dependent; for example, transgenic
96 experiments in *A. thaliana* Col-0 failed to produce self-incompatible plants, whereas experiments
97 using *A. thaliana* C24 were very successful (Nasrallah et al., 2002; Boggs et al., 2009; Iwano et
98 al., 2015; Rozier et al., 2020). The cause of this was linked to inverted repeats within the *A.*
99 *thaliana SRKA* pseudogene which triggers RNA silencing of the introduced *SRK* transgenes
100 (Fujii et al., 2020). For the Col-0 accession, the inverted repeat was found in a conserved region
101 of the predicted *pseudoSRKA* kinase domain resulting in the silencing of closely related *SRK*
102 transgenes. For the C24 accession, the inverted repeat was found in a more polymorphic region
103 of the predicted *pseudoSRKA* ectodomain and appeared to be less effective at inducing RNA
104 silencing of related *SRK* transgenes (Fujii et al., 2020).
105 We have found that a strong self-incompatibility response can also be recapitulated in *A.*
106 *thaliana* Col-0 when the *A. lyrata* or *A. halleri ARC1* transgene was added along with the *A.*
107 *lyrata* or *A. halleri SP11/SCR* and *SRK* transgenes (Indriolo et al., 2014; Zhang et al., 2019). The
108 ARC1 E3 ubiquitin ligase is proposed to act directly downstream of SRK in the self-
109 incompatibility signaling pathway (Gu et al., 1998; Stone et al., 1999; Stone et al., 2003). A large
110 part of the *ARC1* gene has been deleted in the *A. thaliana* genome, and knockdowns of *ARC1* in
111 self-incompatible *Brassica napus* and *A. lyrata* resulted in a partial breakdown of self-
112 incompatibility (Stone et al., 1999; Indriolo et al., 2012). ARC1 is proposed to target cellular
113 components that are required in the stigma to accept compatible pollen, such as the EXO70A1
114 exocyst subunit (Samuel et al., 2009) and *Brassica* GLO1 (Sankaranarayanan et al., 2015). Self-
115 incompatible pollinations also induced a strong and rapid cytosolic calcium influx in the
116 stigmatic papillae (Iwano et al., 2015). These combined self-incompatibility responses are
117 proposed to disrupt the secretory activity in the stigmatic papillae which would be required for
118 compatible pollen acceptance (Dickinson, 1995; Elleman and Dickinson, 1996; Samuel et al.,
119 2009; Safavian and Goring, 2013; Safavian et al., 2015; Goring, 2017).
120 In previous work, we uncovered signs of autophagy activation in *A. lyrata* and *A. thaliana*
121 stigmatic papillae within 10 minutes of self-incompatible pollinations, but not with compatible
122 pollinations (Safavian and Goring, 2013; Indriolo et al., 2014). TEM images revealed structures

123 resembling autophagic bodies in the vacuoles of stigmatic papilla following self-incompatible
124 pollinations (Safavian and Goring, 2013; Indriolo et al., 2014). In contrast, TEM images of
125 compatible pollinations revealed vesicle-like structures in the stigmatic papillae under the
126 compatible pollen contact site suggestive of secretory activity (Safavian and Goring, 2013;
127 Indriolo et al., 2014). The presence of autophagosomes in *A. lyrata* self-incompatible
128 pollinations was further confirmed using the GFP-ATG8a autophagosome marker (Safavian and
129 Goring, 2013). Although these studies indicated that autophagy was activated following self-
130 incompatible pollinations, it was unclear whether autophagy is essential for the rejection of self-
131 incompatible pollen. Here, we have used two different self-incompatible (SI) transgenic *A.*
132 *thaliana* lines (in the Col-0 and C24 accessions; Iwano et al., 2014; Zhang et al., 2019) to test the
133 requirement of the autophagy system for self-pollen rejection. When loss-of-function mutants in
134 the *AUTOPHAGY7* (*ATG7*) and *AUTOPHAGY5(ATG5)* genes (Chung et al., 2010; Ding et al.,
135 2018) were combined with the SI-Col-0 and SI-C24 lines, we observed a partial breakdown of
136 the self-incompatibility response in both accessions. This indicates that autophagic activity is
137 required for the effective rejection of self-incompatible pollen, and thus, elucidates an additional
138 downstream cellular event in the self-incompatibility pathway.
139
140 **Results**
141 **Generation of self-incompatible *A. thaliana* transgenic lines carrying the *atg7* and *atg5***
142 **mutations to disrupt autophagy**
143 To investigate the involvement of autophagy in self-incompatibility, two different transgenic *A.*
144 *thaliana* SI lines were used to cross with *atg7* and *atg5* autophagy mutants. ATG7 and ATG5 are
145 essential components in the formation of autophagosomes (reviewed in Ding et al., 2018), and
146 both the *atg7* and *atg5* mutations lead to a loss of autophagy (Thompson et al., 2005; Chung et
147 al., 2010; Young et al., 2019). The first self-incompatible line is in the Col-0 accession (SI-Col-
148 0) and carries the *A. halleri SCR13*, *SRK13* and *ARC1* transgenes in a single T-DNA (*Ah-SCR13*
149 *Ah-SRK13 Ah-ARC1* #2 line; Zhang et al., 2019). This SI-Col-0 line was crossed to the
150 previously characterized *atg7-2* mutant in the Col-0 accession (Chung et al., 2010). The F_1 plants
151 from this cross were selfed, and all pollination assays were carried out in the F_2 generation. To
152 confirm that any observed effects were not specific to the loss of *ATG7*, the previously
153 characterized *atg5-1* mutation in the Col-0 accession (Thompson et al., 2005) was also crossed

154 into the SI-Col-0 line, and taken to the F_2 generation for pollination assays. The second self-
155 incompatible line is in the C24 accession (SI-C24) and carries the *A. lyrata SCRb* and *SRKb*
156 transgenes (SI-C24 #15-1 line; Iwano et al., 2015). As there were no *atg7* mutants available in
157 the C24 accession, CRISPR/Cas9 technology was used to generate additional *atg7* mutants.
158 Deletion of the *ATG7* gene was confirmed through PCR and sequencing of genomic regions
159 flanking gRNA target sites (Supplemental Fig. S1). The *atg7-9* C24 mutant displayed the same
160 overall wild-type plant and flower morphology (Supplemental Fig. S2) as seen for the *atg7-2*
161 Col-0 mutant. The C24 *atg7-9* mutant was crossed with the SI-C24 line, and following selfing of
162 the F_1 plants, all pollination assays were carried out in F_2 generation (T_4 generation for the *atg7-*
163 *9* mutation). For all three sets of F_2 progeny, genotyping was first carried out to identify the
164 transgenic plants carrying the SI transgenes, followed by genotyping for the *atg7* or atg5
165 mutations to identify plants that were wild-type or homozygous for the *atg* mutations.
166
167 **Disrupting autophagy breaks down the initial self-incompatible response of blocking pollen**
168 **hydration**
169 To assess the early stages of pollen rejection, the pollen hydration checkpoint was first
170 investigated. Self-incompatible pollen from the parental SI-Col-0 or SI-C24 transgenic lines
171 were used to pollinate pistils from the respective F_2 progeny segregating for the *atg7* or *atg5*
172 mutations, and pollen hydration assays were carried out by measuring the increase in pollen
173 diameter at 10 min post-pollination (Lee et al., 2020). Positive controls of the SI-Col-0 and SI-
174 C24 pollen placed on compatible wildtype Col-0 and C24 pistils, respectively, resulted in a large
175 increase in diameter as a result of pollen hydration (Fig. 1A, B). In contrast, self-pollen placed on
176 the SI-Col-0 and SI-C24 pistils resulted in very little pollen hydration at 10-minutes post-
177 pollination (Fig. 1A, B). This lack of hydration was consistent between the SI-Col-0 and SI-C24
178 lines and indicative of the early recognition and rejection of self-incompatible pollen.
179 Importantly, stigmas from the *atg7-2, atg5-1 and atg7-9* mutants showed normal SI-Col-0 and
180 SI-C24 pollen hydration, respectively, indicating that disruption in the autophagic process did
181 not perturb the compatible post-pollination responses (Fig. 1A, B).
182 For the F_2 progeny from the SI-Col-0 x *atg7-2* cross, the SI-Col-0 plants homozygous for
183 wildtype *ATG7* showed the same small increase in pollen hydration as the control self-
184 incompatible pollinations at 10 min post-pollination. In contrast, when SI-Col-0 pollen was

185 applied to the SI-Col-0 stigmas that were homozygous for the *atg7-2* mutation, an increase in
186 pollen hydration was observed, indicating an incomplete rejection of the self-incompatible pollen
187 (Fig. 1A). Similarly, pollen hydration assays on the F_2 progeny from the SI-Col-0 x *atg5-1* cross
188 showed that hydration of SI-Col-0 pollen on SI-Col-0 stigmas wild-type for *ATG5* displayed a
189 small increase while SI-Col-0 pollen hydration on SI-Col-0 stigmas homozygous for the *atg5-1*
190 mutation was significantly increased (Fig. 1B). A comparable set of pollen hydration
191 experiments on the F_2 progeny from the SI-C24 x *atg7-9* cross also showed a similar trend (Fig.
192 1C). SI-C24 stigmas that were wild-type for *ATG7* supported similar small increases in SI-C24
193 pollen hydration as the control self-incompatible pollinations, and the introduction of the *atg7-9*
194 mutation into this background resulted in increased hydration of the self-incompatible pollen.
195 Together, these results indicate that autophagy is required to fully prevent the hydration of self-
196 incompatible pollen.
197
198 **Disruption of autophagy increases self-incompatible pollen tube penetration**
199 With the observed increase in self-incompatible pollen hydration, the next stage of preventing
200 self-incompatible pollen germination and pollen tube penetration was investigated. To determine
201 if this block was affected by the *atg7* and *atg5* mutations, pollinated pistils were collected at 2-
202 and 24-hours post-pollination and stained with aniline blue to visualize pollen tubes. At 2-hours
203 post-pollination, SI-Col-0 and SI-C24 pollen was completely rejected by the respective self-
204 incompatible pistils, and no pollen tubes were visible (Supplemental Fig. S2 and S3). Although
205 we did not see any obvious difference at 2-hours post-pollination, we did observe an occasional
206 pollen tube that penetrated the stigma barrier of the SI-Col-0 and SI-C24 *atg* homozygous
207 mutants. To address whether we could observe a greater number of SI-Col-0 and SI-C24 pollen
208 tubes after a longer period, pollinated pistil samples were then harvested at 24-hours post-
209 pollination. A later time point following pollination is more reflective of the natural pollination
210 process and provides more time for the self-incompatible pollen to germinate and grow into the
211 pistil. Self-pollination of the SI-Col-0 and SI-C24 parental lines resulted in an absence of pollen
212 tubes (Fig. 2A, 3A and 4A) while pollinations with compatible wild-type pollen led to an
213 abundance of pollen tubes growing in the pistils (Fig. 2B, 3B and 4B). The results indicated that
214 the SI-Col-0 and SI-C24 were able to fully reject self-incompatible pollen and accept wild-type
215 compatible pollen at 24-hours post-pollination. The SI-Col-0 and SI-C24 pollen also produced

216 numerous pollen tubes when placed on the *atg* mutant pistils, indicating that the absence of
217 autophagy did not affect these compatible pollinations (Fig. 2C and 3C). The impact of the *atg*
218 mutations on self-incompatibility at 24-hours post-pollination was examined by applying the SI-
219 Col-0 and SI-C24 pollen on their respective F_2 progeny homozygous for the *atg* mutations.
220 When SI-Col-0 *atg7-2* stigmas or SI-Col-0 *atg5-1* stigmas were pollinated with SI-Col-0 pollen,
221 there was a general increase in the number of pollen grains adhering to the stigma and forming
222 pollen tubes when compared to the SI-Col-0 pistils (Fig. 2D-F and 3D-F). The pollinations were
223 repeated for the SI-C24 F_2 plants, and again the SI-C24 *atg7-9* pistils did show some SI-C24
224 pollen adhering to the stigmatic surface and successfully growing pollen tubes through the pistil
225 while the SI-C24 *ATG7* pistils rejected the SI-C24 pollen (Fig. 4D-F). The number of pollen
226 tubes were counted in the SI-Col-0 and SI-C24 pistils that were wild-type or homozygous for the
227 *atg* mutations, and a significant increase in the number of pollen tubes were counted in the
228 homozygous *atg7* and *atg5* mutants (Fig. 2F, 3F and 4F). Thus, the 24-hours post-pollination
229 samples demonstrated that autophagy is required for fully blocking self-incompatible pollen
230 germination and pollen tube growth through the self-incompatible pistil.
231
232 **Loss of autophagy increases seed set in the self-incompatible lines**
233 With the observation that self-incompatibility is partially lost in the SI-Col-0 *atg7-2*, SI-Col-0
234 *atg5-1* and SI-C24 *atg7-9* mutant pistils, resulting in more pollen tubes growing through the
235 pistils, the impact of this on seed set was assessed. Manual pollinations were carried out using
236 SI-Col-0 and SI-C24 pollen on pistils from the respective parental lines and F_2 progeny
237 homozygous for the *atg7* or *atg5* mutations, and 2-week old siliques were harvested for seed
238 counting (Fig. 5; Supplemental Fig. S5). As expected for compatible pollinations in Col-0, C24,
239 and the *atg* mutants, abundant seeds/silique were produced (Fig. 5A-C). As well, self-
240 pollinations of SI-Col-0 and SI-C24 pistils resulted in a very limited seed yield consistent with
241 the rejection of self-incompatible pollen (Fig. 5A-C). When the SI-Col-0 *atg7-2* pistils were
242 pollinated with SI-Col-0 pollen, there was a significant increase in yield to 27 seeds/silique
243 compared to 12.8 seeds/silique for SI-Col-0 indicating an incomplete rejection of the SI-Col-0
244 pollen by the SI-Col-0 *atg7-2* pistils (Fig. 5A). Similarly, when SI-Col-0 *atg5-1* pistils were
245 pollinated with SI-Col-0 pollen, there was an increased average yield of 31.9 seeds/silique
246 compared to 10.8 seeds/silique for SI-Col-0 (Fig. 4B). Finally, similar trends in seed yields were

247 observed in the C24 accession. Self-incompatible pollinations with SI-C24 pistils resulted in a
248 low average of 6.8 seeds/silique as expected yet when the SI-C24 *atg7-9* pistils were pollinated
249 with SI-C24 pollen, there was a significant increase in seed yields to17.2 seeds/silique (Fig. 5C).
250 Altogether, these results indicate that loss of autophagy was sufficient to disrupt the self-
251 incompatibility pathway allowing for the growth of more SI pollen tubes through the SI-Col-0
252 and SI-C24 pistils carrying *atg7* or *atg5* mutations to initiate fertilization and seed production,
253 and thus, confirming that autophagy is required for full rejection of self-pollen.
254
255
256 **Autophagosomes are produced following self-pollination in the SI-C24 line**
257 Previously, autophagosomes were detected by TEM following self-incompatible pollinations in
258 *A. lyrata* and in the transgenic self-incompatible *A. thaliana* in the Col-0 accession transformed
259 with *A. lyrata* S-locus genes (Safavian and Goring, 2013; Indriolo et al., 2014). To confirm that
260 autophagosomes are also forming in the SI-Col-0 *Ah-SCR13 Ah-SRK13 Ah-ARC1* #2 line used in
261 this study, *GFP-ATG8a* was used as an autophagosome marker (Thompson et al., 2005). Col-0
262 plants carrying the *ProUBQ10:GFP-ATG8a* construct (Kim et al., 2013) were crossed with the
263 SI-Col-0 line, and the subsequent F_1 generation was used for imaging. The SI-Col-0 *GFP-*
264 *ATG8a* stigmas were imaged as unpollinated or manually pollinated with SI-Col-0 pollen. At 15-
265 minutes post-pollination, many GFP punctae were observed in the SI-Col-0 *GFP-ATG8a*
266 stigmatic papillae contacting SI-Col-0 pollen (Fig. 6A). Conversely, few puncta were observed
267 in unpollinated SI-Col-0 GFP-ATG8a stigmatic papillae, consistent with a low background level
268 of autophagy (Fig. 6C). The number of puncta were counted for both SI-Col-0 pollinated and
269 unpollinated SI-Col-0 GFP-ATG8a stigmatic papillae (Fig. 6E), and there was a significant
270 increase in the number of GFP-ATG8a-labelled punctae in the SI-pollinated SI-Col-0 *GFP-*
271 *ATG8a* stigmatic papillae indicated a strong induction of autophagy. These observations confirm
272 our previous findings that autophagy is activated in the stigmatic papillae with self-incompatible
273 pollinations when compared to an unpollinated stigma (Safavian and Goring, 2013; Indriolo and
274 Goring, 2014).
275
276 **Discussion**

277 Self-incompatibility plays an important regulatory role in many outcrossing Brassicaceae species
278 where producing inbred progeny would be disadvantageous (Shimizu and Tsuchimatsu, 2015;
279 Durand et al., 2020). Previous studies have uncovered many important steps in the self-
280 incompatibility pathway, but there are still outstanding questions on the cellular mechanisms by
281 which self-pollen is rejected (reviewed in Doucet et al., 2016; Goring, 2017; Jany et al., 2019). In
282 previous studies, we observed the presence of autophagosomes in the cytoplasm and autophagic
283 bodies in the vacuole with self-incompatible pollinations in self-incompatible *A. lyrata* and
284 transgenic self-incompatible *A. thaliana* Col-0 (Safavian and Goring, 2013; Indriolo and Goring,
285 2014). What was not known, however, was whether autophagy was necessary for self-
286 incompatible pollen rejection. In this study, we addressed this question by crossing two different
287 autophagy-deficient mutants (*atg7* and *atg5*) into two different transgenic self-incompatible *A.*
288 *thaliana* lines, and demonstrated that a functioning autophagy system is required in the stigma
289 for the full rejection of self-incompatible pollen. It is important to note that disrupting autophagy
290 did not cause a full loss of self-incompatibility indicating that other cellular responses are
291 required in conjunction with autophagy for self-incompatible pollen rejection. Importantly, this
292 partial breakdown in the stigma was seen for all stages from increased pollen hydration to more
293 pollen tubes growing through pistil to increase seed yields. Finally, the requirement of autophagy
294 in the rejection of self-incompatible pollen was consistent between the three different autophagy
295 deficient mutants *(atg7-2, atg7-9* and *atg5)* and the two different *Arabidopsis thaliana*
296 accessions (Col-0 and C24) used in the SI lines indicating that there is a shared mechanism for
297 self-incompatible pollen rejection.
298 The rationale for using both the SI-Col-0 and SI-C24 lines was to determine if there were any
299 accession- or transgene-specific associations with autophagy. The SI-Col-0 carries the *A. halleri*
300 *SCR13*, *SRK13* and *ARC1* transgenes (Zhang et al., 2019) while the SI-C24 line carries the *A.*
301 *lyrata SCRb* and *SRKb* transgenes (Iwano et al., 2015). In addition to two different S-haplotypes
302 from two different *Arabidopsis* species, the SI-Col-0 line also carries the *A. halleri ARC1*
303 transgene. The fact that both accessions require an intact autophagy system in the stigma for full
304 self-incompatible pollen rejection indicates that autophagy activation does not require ARC1,
305 though the potential involvement of another related PUB E3 ligase cannot be ruled out (Indriolo
306 et al., 2012; Indriolo and Goring, 2016). Our results indicate that autophagy is a clear
307 commonality in the self-incompatibility response between these two accessions, although

308 variation may exist in the execution of this cellular function. The question then arises to the
309 purpose of autophagy activation in self-incompatibility.
310 Self-incompatible pollen carries the signals to be recognized as both self-incompatible pollen and
311 compatible pollen, and it has been hypothesized that self-incompatibility blocks compatible
312 pollen responses in the stigma (Dickinson, 1995). With the working model that secretory activity
313 in the stigma is required for compatible pollen acceptance (reviewed in Dickinson, 1995; Doucet
314 et al., 2016; Goring, 2017), several of the self-incompatibility cellular responses such as
315 EX070A1 inhibition (Samuel et al., 2009; Sankaranarayanan et al., 2015), a strong and rapid
316 calcium influx (Iwano et al., 2015), and the absence of actin focalization (Rozier et al., 2020) are
317 consistent with blocking secretion (reviewed in Goring, 2017). Autophagy could also be an
318 additional step to clear any secretory activity that was initially activated. Another possibility is
319 that autophagy is resetting the cellular program to reject self-pollen. (Rodriguez et al., 2020)
320 recently demonstrated a role for autophagy in switching *A. thaliana* cell fate determination
321 following treatments with different signals. Autophagy was shown to be required for this switch
322 and was proposed to "clean-up" the cell to allow for the new cellular program to be established.
323 In the context of self-incompatibility, autophagy activation in the stigma could be linked to
324 reprogramming the cells from the default compatible pollen responses to the self-pollen rejection
325 pathway.
326 In conclusion, this study now firmly places autophagy as part of the cellular mechanisms leading
327 to self-incompatible pollen rejection. Future studies will need to focus on how autophagy is
328 activated in the self-incompatibility pathway and whether there are specific cytoplasmic
329 components targeted for autophagic destruction. Understanding the mechanisms underlying self-
330 incompatibility is important as seed yield of many important crop species is directly tied to their
331 reproductive success, and the ability to modulate selfing would be a powerful tool in increasing
332 yield.
333
334 **Materials and methods**
335 **Plant materials and growth conditions**
336 All *Arabidopsis thaliana* seeds (Col-0, C24, transgenic lines, T-DNA insertion mutants and
337 CRISPR/Cas9 deletion mutants) were sterilized and cold stratified at 4°C for 3 days. Seedlings
338 were germinated on ½ Murashige and Skoog (MS) medium plates supplemented with 0.4 (w/v)

339 phytoagar (pH 5.8) and 1% (w/v) sucrose. Seedlings were grown at 22°C under 16h light for 7
340 days, and then transferred to Sunshine #1 soil supplemented with Plant Prod All Purpose
341 Fertilizer 20-20-20 (1g/L water). All plants were grown in chambers under a 16-hour light/8-
342 hour dark growth cycle at 22°C, with humidity kept under 50%.
343 For the Col-0 accession experiments, the *Ah-SCR13 Ah-SRK13 Ah-ARC1* #2 Col-0 line (Zhang et
344 al., 2019) was crossed to the *atg7-2* mutant (Col-0 accession; Chung et al., 2010) and *atg5-1*
345 mutant (Thompson et al., 2005). For the C24 accession experiments, the *SI-C24 #15-1* line (with
346 *Al-SCRb AlSRKb*; Iwano et al., 2015) was crossed to the *atg7-9* mutant (C24 accession; see
347 below). All transgenic lines were genotyped using primers found in Supplemental Table 1. For
348 the C24 accession, plants were genotyped for $AlSCR_b$, $AlSRK_b$ and *atg7-9*. Progeny were
349 analyzed in the F_2 generation for all three crosses. For SI-Col-0 *GFP-ATG8a*, the *Ah-SCR13 Ah-*
350 *SRK13 Ah-ARC1 #2* Col-0 line (Zhang et al., 2019), was crossed into the *ProUBQ10:GFP-*
351 *ATG8a* line (Col-0 accession; Kim et al., 2013), and the resulting F_1 progeny was used for all
352 imaging.
353
354 **Plasmid construction and plant transformation**
355 The *atg7-9* CRISPR/Cas9 deletion mutation was generated in C24 using previously described
356 methods in the Col-0 accession (Doucet et al., 2019; Doucet et al., 2019). The final pBEE401E
357 vector contained two guide RNAs targeting exons 3 and 8 of *ATG7* (Supplemental Fig. S1).
358 *Arabidopsis thaliana* C24 plants were transformed using floral dip (Clough and Bent, 1998), and
359 plants were dipped twice, 3 days apart, to maximize transformation efficiency. T1 seeds were
360 collected and germinated on soil, and one-week old seedlings were sprayed with BASTA
361 herbicide to select for transformants. PCR was used to confirm transformants (BASTA marker)
362 and the presence of *atg7* mutations (deletions of the exon 3-8 region; Supplemental Figure S1).
363 These *atg7* deletion mutants were then verified through sequencing of regions flanking the
364 deletions. The *atg7* mutants showed a wild-type plant and flower morphology, along with the
365 shorter life span typically seen in *atg* mutants (Thompson et al., 2005; Avila-Ospina et al., 2014).
366 One homozygous mutant, *atg7-9*, from the T2 generation was crossed to the *SI-C24 #15-1* line,
367 and all data was collected in the F_2 generation of this cross (F_4 generation for *atg7-9*).
368
369 **Confocal Microscopy**

370 *A. thaliana* SI-Col-0 plants carrying the *ProUBQ10:GFP-ATG8a* construct were manually
371 pollinated using pollen from the self-incompatible SI-Col-0 line. Pistils were removed at 10-
372 minutes post-pollination and images of autophagosomes were taken at 15-minutes post-
373 pollination. All images were taken using a Leica SP8 confocal microscope, with standard GFP
374 excitation-emission wavelengths (488nm excitation, 495-545nm emission) with a pinhole
375 diameter of 2.0AU. Leica LAS AF lite in combination with ImageJ was used for image
376 processing and puncta counting. GFP punctae were counted in stigmatic papillae cell areas
377 directly adjacent to SI-Col-0 pollen, and an equivalent cell area in unpollinated samples.
378
379 **Assays for Pollen hydration, Aniline blue staining, and Seed set**
380 All post-pollination assays used manual pollinations and were conducted as described in Lee et
381 al., 2020). For the SI-C24 plants, late stage 12 pistils were first emasculated and wrapped in
382 plastic wrap overnight prior to pollination. For the SI-Col-0 plants, the pistils did not require
383 emasculation due to the approach herkogamy phenotype (Zhang et al. 2019*)*, and freshly opened
384 flowers with unpollinated pistils were selected for these assays. All pollinations were completed
385 at humidity levels under 50% for consistency. Pollen hydration assays were conducted by
386 removing and mounting pistils on ½ MS, and lightly pollinating the stigmatic surface using a
387 single anther. Images were taken at 0- and 10-min post-pollination using a Nikon sMz800
388 microscope, and pollen grains on the stigmatic surface were randomly selected for measurements
389 using the NIS-elements imaging software. For the aniline blue staining, one anther was used to
390 lightly pollinate each pistil, and the pistils were then collected at 2- and 24-hours post-pollination
391 for staining as described in Lee et al., 2020). The aniline blue-stained pistils were mounted on a
392 slide with sterile water, flattened, and imaged using a Zeiss Axioscope2 Plus fluorescent
393 microscope. For seeds counts, pistils were manually pollinated with a single anther and were left
394 for 10-14 days. The maturing siliques were then removed and cleared in 70% (v/v) ethanol for 3-
395 5 days, or until seeds were visible (Beuder et al., 2020). Siliques were then mounted on a dry
396 slide with the septum facing upwards and imaged using a Nikon sMz800 microscope, and seeds
397 were counted using the NIS-elements imaging software.
398
399
400

401 **Supplemental Material**

402 **Supplemental Figure S1.** Generation of the *ATG7* CRISPR/Cas9 deletion mutation in the C24
403 accession.

404 **Supplemental Figure S2**. Representative images of flowering plants for the SI-C24 and *atg7-9*
405 mutant plants in the C24 accession.

406 **Supplemental Figure S3**. Representative images of aniline blue-stained pistils at 2 hrs following
407 pollination with SI-Col-0 or Col-0 pollen.

408 **Supplemental Figure S4**. Representative images of aniline blue-stained pistils at 2 hrs following
409 pollination with SI-C24 or C24 pollen.

410 **Supplemental Figure S5.** Representative images of cleared siliques used in seed counting for
411 control and SI plants with the *atg7* mutation.

412 **Supplemental Table 1.** Primer Sequences.

413

414

415

416 **Acknowledgements**

417 We thank Laura Canales and Arjun Sharma for technical assistance, and members of the Goring
418 lab for critically reading this article. We are very grateful to Seiji Takayama (Nara Institute of
419 Science and Technology; University of Tokyo) for providing the *SI-C24 #15-1* seeds (*A. thaliana*
420 C24), Richard Vierstra (Washington University in St Louis) and Peter Bozhkov (Swedish
421 University of Agricultural Sciences) for providing *atg7-2* and *atg5-1* mutant seeds (*A. thaliana*
422 Col-0), and Marisa Otegui (University of Wisconsin-Madison) for providing the
423 *ProUBQ10:GFP-ATG8a* seeds (*A. thaliana* Col-0).

424

425 **Figure 1. Pollen hydration assays on control and SI F_2 progeny segregating for the *atg7* and**
426 ***atg5* mutations.**
427 Pollen hydration assays for **A,** SI-Col-0 pollen grains placed on stigmas from Col-0, SI-Col-0,
428 *atg7-2*, and F_2 progeny from the SI-Col-0 x *atg7-2* cross; **B,** SI-Col-0 pollen grains placed on
429 stigmas from Col-0, SI-Col-0, *atg5-1*, and F_2 progeny from the SI-Col-0 x *atg5-1* cross; and **C,**
430 SI-C24 pollen grains placed on stigmas from C24, SI-C24, *atg7-9*, and F_2 progeny stigmas from
431 the SI-C24 x *atg7-9* cross. Pollen hydration was measured by taking pollen grain diameters at 0-
432 and 10-minutes post-pollination. Data is shown as Mean +/- SE with all data points displayed.
433 n=30 pollen grains per line, $P<0.05$ (One-way ANOVA with Tukey-HSD post-hoc test).
434
435 **Figure 2. Representative images of aniline blue-stained SI-Col-0 or SI-Col-0 *atg7-2* pistils at**
436 **24 hrs following pollination.**
437 **A-E**, All stigmas were hand-pollinated with SI-Col-0 pollen or wild-type Col-0 pollen as
438 indicated and collected at 24 hours post-pollination for aniline blue staining. The genotypes of
439 the pistils are indicated for each panel. Pollen tubes penetrating through the stigma and style
440 indicate a breakdown of self-incompatibility as seen in **E**. For each panel, top image =
441 brightfield, bottom image = aniline blue. Scale bar = 100µm
442 **F**, Bar graph showing the mean number of pollen tubes at 24 hrs post-pollination. Data is shown
443 as Mean +/- SE with all data points displayed. n = 11-12 pistils per line. At 24 hours, pistils
444 from SI-Col-0 *atg7-2* mutants allowed a significantly higher number of SI-Col-0 pollen tubes
445 compared to the SI-Col-0 pistils ($P<0.05$).
446
447 **Figure 3. Representative images of aniline blue-stained SI-Col-0 or SI-Col-0 *atg5-1* pistils at**
448 **24 hrs following pollination.**
449 **A-E**, All stigmas were hand-pollinated with SI-Col-0 pollen or wild-type Col-0 pollen as
450 indicated and collected at 24 hours post-pollination for aniline blue staining. The genotypes of
451 the pistils are indicated for each panel. Pollen tubes penetrating through the stigma and style
452 indicate a breakdown of self-incompatibility as seen in **E**. For each panel, top image =
453 brightfield, bottom image = aniline blue. Scale bar = 100µm
454 **F**, Bar graph showing the mean number of pollen tubes at 24 hrs post-pollination. Data is shown
455 as Mean +/- SE with all data points displayed. n = 10 pistils per line. At 24 hours, pistils from

456 SI-Col-0 *atg5-1* mutants allowed a significantly higher number of SI-Col-0 pollen tubes
457 compared to the SI-Col-0 pistils ($P<0.05$).
458
459 **Figure 4. Representative images of aniline blue-stained SI-C24 or SI-C24 *atg7-9* pistils at 24**
460 **hrs following pollination.**
461 **A-E,** All stigmas were hand-pollinated with SI-C24 pollen or wild-type C24 pollen as indicated
462 and collected at 24 hours post-pollination for aniline blue staining. The genotypes of the pistils
463 are indicated for each panel. Pollen tubes penetrating through the stigma and style indicate a
464 breakdown of self-incompatibility as seen in **E**. For each panel, top image = brightfield, bottom
465 image = aniline blue. Scale bar = 100µm
466 **F,** Bar graph showing the mean number of pollen tubes at 24 hrs post-pollination. Data is shown
467 as Mean +/- SE with all data points displayed. n = 8-10 pistils per line. At 24 hours, pistils from
468 SI-C24 *atg7-9* mutants allowed a significantly higher number of SI-C24 pollen tubes compared
469 to the SI-C24 pistils ($P<0.05$).
470
471 **Figure 5. Seeds per silique counts for control and SI F_2 progeny with the *atg7* or *atg5***
472 **mutations.**
473 Seeds per silique counts following manual pollination with **A, B,** SI-Col-0 pollen or **C,** SI-C24
474 pollen on pistils with the indicated genotypes. Siliques were harvested at 2-weeks post-
475 pollination and cleared for seeds counts. Data is shown as Mean +/- SE with all data points
476 displayed. n= 8-10 siliques per line. Compared to the control SI pollinations, significant
477 increases in the number of seeds per silique were observed for the SI plants that were
478 homozygous for the *atg7* or *atg5* mutations, $P<0.05$ (One-way ANOVA with Tukey-HSD post-
479 hoc test).
480
481 **Figure 6. Autophagosomes are more abundant in SI-Col-0 *GFP-ATG8a* papillae following**
482 **pollination with SI-Col-0 pollen.**
483 More autophagosomes marked by GFP-ATG8a are visible at 15-minutes post-pollination in the
484 SI-Col-0 *GFP-ATG8a* papillae (**A-B**) compared to unpollinated SI-Col-0 *GFP-ATG8a* papillae
485 (**C-D**). Scale bar = 10µm.

486 **E**, Bar graph showing the mean number of autophagosomes present in each sample. Data is
487 shown as Mean +/- SE with all data points displayed. n=14 papillae. At 15 min post-pollination
488 with SI-Col-0 pollen, there is a significant increase in the number of GFP-labelled punctae in the
489 SI-Col-0 *GFP-ATG8a* papillae ($P<0.05$). The large punctae are chloroplasts with
490 autofluorescence and were not counted.
491

492 **Literature Cited**

493 Adhikari PB, Liu X, Wu X, Zhu S, Kasahara RD (2020) Fertilization in flowering plants: an
494 odyssey of sperm cell delivery. Plant Mol Biol 103: 9-32
495 Avila-Ospina L, Moison M, Yoshimoto K, Masclaux-Daubresse C (2014) Autophagy, plant
496 senescence, and nutrient recycling. J Exp Bot 65: 3799-3811
497 Beuder S, Dorchak A, Bhide A, Moeller SR, Petersen BL, MacAlister CA (2020) Exocyst
498 mutants suppress pollen tube growth and cell wall structural defects of hydroxyproline O-
499 arabinosyltransferase mutants. Plant J
500 Boggs NA, Nasrallah JB, Nasrallah ME (2009) Independent S-Locus Mutations Caused Self-
501 Fertility in Arabidopsis thaliana. Plos Genetics 5
502 Chung T, Phillips AR, Vierstra RD (2010) ATG8 lipidation and ATG8-mediated autophagy in
503 Arabidopsis require ATG12 expressed from the differentially controlled ATG12A AND
504 ATG12B loci. Plant J 62: 483-493
505 Clough SJ, Bent AF (1998) Floral dip: A simplified method for Agrobacterium-mediated
506 transformation of Arabidopsis thaliana. Plant Journal 16: 735-743
507 Dickinson H (1995) Dry stigmas, water and self-incompatibility in Brassica. Sexual Plant
508 Reproduction 8: 1-10
509 Ding X, Zhang X, Otegui MS (2018) Plant autophagy: new flavors on the menu. Curr Opin Plant
510 Biol 46: 113-121
511 Doucet J, Lee HK, Goring DR (2016) Pollen acceptance or rejection: a tale of two pathways.
512 Trends in plant science 21: 1058-1067
513 Doucet J, Lee HK, Udugama N, Xu J, Qi B, Goring DR (2019) Investigations into a putative role
514 for the novel BRASSIKIN pseudokinases in compatible pollen-stigma interactions in
515 Arabidopsis thaliana. BMC Plant Biol 19: 549
516 Doucet J, Truong C, Frank-Webb E, Lee HK, Daneva A, Gao Z, Nowack MK, Goring DR
517 (2019) Identification of a role for an E6-like 1 gene in early pollen-stigma interactions in
518 Arabidopsis thaliana. Plant Reprod 32: 307-322
519 Durand E, Chantreau M, Le Veve A, Stetsenko R, Dubin M, Genete M, Llaurens V, Poux C,
520 Roux C, Billiard S, Vekemans X, Castric V (2020) Evolution of self-incompatibility in
521 the Brassicaceae: Lessons from a textbook example of natural selection. Evol Appl 13:
522 1279-1297

523 Elleman C, Dickinson H (1996) Identification of pollen of components regulating the responses
524 in stigmatic Brassica oleracea. New Phytologist 133: 197-205
525 Fujii S, Shimosato-Asano H, Kakita M, Kitanishi T, Iwano M, Takayama S (2020) Parallel
526 evolution of dominant pistil-side self-incompatibility suppressors in Arabidopsis. Nat
527 Commun 11: 1404
528 Goring DR (2017) Exocyst, exosomes, and autophagy in the regulation of Brassicaceae pollen-
529 stigma interactions. J Exp Bot 69: 69-78
530 Goubet PM, Berges H, Bellec A, Prat E, Helmstetter N, Mangenot S, Gallina S, Holl AC, Fobis-
531 Loisy I, Vekemans X, Castric V (2012) Contrasted patterns of molecular evolution in
532 dominant and recessive self-incompatibility haplotypes in Arabidopsis. PLoS Genet 8:
533 e1002495
534 Gu T, Mazzurco M, Sulaman W, Matias DD, Goring DR (1998) Binding of an arm repeat
535 protein to the kinase domain of the S-locus receptor kinase. Proceedings of
536 the National Academy of Sciences 95: 382-387
537 Guo YL, Zhao X, Lanz C, Weigel D (2011) Evolution of the S-locus region in Arabidopsis
538 relatives. Plant Physiol 157: 937-946
539 Indriolo E, Goring DR (2014) A conserved role for the ARC1 E3 ligase in Brassicaceae self-
540 incompatibility. Front Plant Sci 5: 181
541 Indriolo E, Goring DR (2016) Yeast two-hybrid interactions between Arabidopsis lyrata S
542 Receptor Kinase and the ARC1 E3 ligase. Plant Signal Behav 11: e1188233
543 Indriolo E, Safavian D, Goring DR (2014) The ARC1 E3 ligase promotes two different self-
544 pollen avoidance traits in Arabidopsis. The Plant Cell 26: 1525-1543
545 Indriolo E, Tharmapalan P, Wright SI, Goring DR (2012) The ARC1 E3 ligase gene is frequently
546 deleted in self-compatible Brassicaceae species and has a conserved role in Arabidopsis
547 lyrata self-pollen rejection. Plant Cell 24: 4607-4620
548 Iwano M, Igarashi M, Tarutani Y, Kaothien-Nakayama P, Nakayama H, Moriyama H, Yakabe
549 R, Entani T, Shimosato-Asano H, Ueki M, Tamiya G, Takayama S (2014) A Pollen
550 Coat–Inducible Autoinhibited Ca²⁺-ATPase Expressed in Stigmatic Papilla
551 Cells Is Required for Compatible Pollination in the Brassicaceae. The Plant Cell 26: 636-
552 649

553 Iwano M, Ito K, Fujii S, Kakita M, Asano-Shimosato H, Igarashi M, Kaothien-Nakayama P,
554 Entani T, Kanatani A, Takehisa M, Tanaka M, Komatsu K, Shiba H, Nagai T, Miyawaki
555 A, Isogai A, Takayama S (2015) Calcium signalling mediates self-incompatibility
556 response in the Brassicaceae. Nat Plants 1: 15128
557 Jany E, Nelles H, Goring DR (2019) The Molecular and Cellular Regulation of Brassicaceae
558 Self-Incompatibility and Self-Pollen Rejection, Vol 343. Elsevier Ltd
559 Johnson MA, Harper JF, Palanivelu R (2019) A Fruitful Journey: Pollen Tube Navigation from
560 Germination to Fertilization. Annual review of plant biology 70: 809-837
561 Kim J, Lee H, Lee HN, Kim SH, Shin KD, Chung T (2013) Autophagy-related proteins are
562 required for degradation of peroxisomes in Arabidopsis hypocotyls during seedling
563 growth. Plant Cell 25: 4956-4966
564 Kusaba M, Dwyer K, Hendershot J, Vrebalov J, Nasrallah JB, Nasrallah ME (2001) Self-
565 Incompatibility in the Genus Arabidopsis: Characterization of the S Locus in the
566 Outcrossing A. Lyrata and Its Autogamous Relative A. Thaliana. The Plant Cell 13: 627-
567 644
568 Lee HK, Macgregor S, Goring DR (2020) A Toolkit for Teasing Apart the Early Stages of
569 Pollen-Stigma Interactions in Arabidopsis thaliana. Methods Mol Biol 2160: 13-28
570 Mizuta Y, Higashiyama T (2018) Chemical signaling for pollen tube guidance at a glance.
571 Journal of Cell Science 131
572 Nasrallah JB (2019) Self-incompatibility in the Brassicaceae: Regulation and mechanism of self-
573 recognition. Curr Top Dev Biol 131: 435-452
574 Nasrallah ME, Liu P, Nasrallah JB (2002) Generation of self-incompatible Arabidopsis thaliana
575 by transfer of two S locus genes from A. lyrata. Science 297: 247-249
576 Nasrallah ME, Liu P, Sherman-Broyles S, Boggs NA, Nasrallah JB (2004) Natural variation in
577 expression of self-incompatibility in Arabidopsis thaliana: Implications for the evolution
578 of selfing. Proceedings of the National Academy of Sciences of the United States of
579 America 101: 16070-16074
580 Palanivelu R, Tsukamoto T (2012) Pathfinding in angiosperm reproduction: pollen tube guidance
581 by pistils ensures successful double fertilization. Wiley Interdisciplinary Reviews:
582 Developmental Biology 1: 96-113

583 Rodriguez E, Chevalier J, Olsen J, Ansbol J, Kapousidou V, Zuo Z, Svenning S, Loefke C,
584 Koemeda S, Drozdowskyj PS, Jez J, Durnberger G, Kuenzl F, Schutzbier M, Mechtler K,
585 Ebstrup EN, Lolle S, Dagdas Y, Petersen M (2020) Autophagy mediates temporary
586 reprogramming and dedifferentiation in plant somatic cells. EMBO J 39: e103315
587 Rozier F, Riglet L, Kodera C, Bayle V, Durand E, Schnabel J, Gaude T, Fobis-Loisy I (2020)
588 Live-cell imaging of early events following pollen perception in self-incompatible
589 Arabidopsis sthaliana. J Exp Bot
590 Safavian D, Goring DR (2013) Secretory activity is rapidly induced in stigmatic papillae by
591 compatible pollen, but inhibited for self-incompatible pollen in the brassicaceae. PLoS
592 ONE 8
593 Safavian D, Zayed Y, Indriolo E, Chapman L, Ahmed A, Goring DR (2015) RNA silencing of
594 exocyst genes in the stigma impairs the acceptance of compatible pollen in Arabidopsis.
595 Plant Physiology 169: 2526-2538
596 Samuel MA, Chong YT, Haasen KE, Aldea-Brydges MG, Stone SL, Goring DR (2009) Cellular
597 pathways regulating responses to compatible and self-incompatible pollen in Brassica and
598 Arabidopsis stigmas intersect at Exo70A1, a putative component of the exocyst complex.
599 Plant Cell 21: 2655-2671
600 Sankaranarayanan S, Jamshed M, Samuel MA (2015) Degradation of glyoxalase I in Brassica
601 napus stigma leads to self-incompatibility response. Nat Plants 1: 15185
602 Schierup MH, Mable BK, Awadalla P, Charlesworth D (2001) Identification and characterization
603 of a polymorphic receptor kinase gene linked to the self-incompatibility locus of
604 Arabidopsis lyrata. Genetics 158: 387-399
605 Shimizu KK, Shimizu-Inatsugi R, Tsuchimatsu T, Purugganan MD (2008) Independent origins
606 of self-compatibility in Arabidopsis thaliana. Mol Ecol 17: 704-714
607 Shimizu KK, Tsuchimatsu T (2015) Evolution of Selfing: Recurrent Patterns in Molecular
608 Adaptation. Annual Review of Ecology, Evolution, and Systematics, Vol 46 46: 593-622
609 Stone SL, Anderson EM, Mullen RT, Goring DR (2003) ARC1 is an E3 ubiquitin ligase and
610 promotes the ubiquitination of proteins during the rejection of self-incompatible Brassica
611 pollen. The Plant Cell 15: 885-898
612 Stone SL, Arnoldo M, Goring DR (1999) A breakdown of Brassica self-incompatibility in ARC1
613 antisense transgenic plants. Science 286: 1729-1731

614 Thompson AR, Doelling JH, Suttangkakul A, Vierstra RD (2005) Autophagic nutrient recycling
615 in Arabidopsis directed by the ATG8 and ATG12 conjugation pathways. Plant Physiol
616 138: 2097-2110
617 Tsuchimatsu T, Goubet PM, Gallina S, Holl AC, Fobis-Loisy I, Berges H, Marande W, Prat E,
618 Meng D, Long Q, Platzer A, Nordborg M, Vekemans X, Castric V (2017) Patterns of
619 Polymorphism at the Self-Incompatibility Locus in 1,083 Arabidopsis thaliana Genomes.
620 Mol Biol Evol 34: 1878-1889
621 Tsuchimatsu T, Suwabe K, Shimizu-Inatsugi R, Isokawa S, Pavlidis P, Stadler T, Suzuki G,
622 Takayama S, Watanabe M, Shimizu KK (2010) Evolution of self-compatibility in
623 Arabidopsis by a mutation in the male specificity gene. Nature 464: 1342-1346
624 Young PG, Passalacqua MJ, Chappell K, Llinas RJ, Bartel B (2019) A facile forward-genetic
625 screen for Arabidopsis autophagy mutants reveals twenty-one loss-of-function mutations
626 disrupting six ATG genes. Autophagy 15: 941-959
627 Zhang T, Zhou G, Goring DR, Liang X, Macgregor S, Dai C, Wen J, Yi B, Shen J, Tu J, Fu T,
628 Ma C (2019) Generation of Transgenic Self-Incompatible Arabidopsis thaliana Shows a
629 Genus-Specific Preference for Self-Incompatibility Genes. Plants (Basel, Switzerland) 8:
630 570

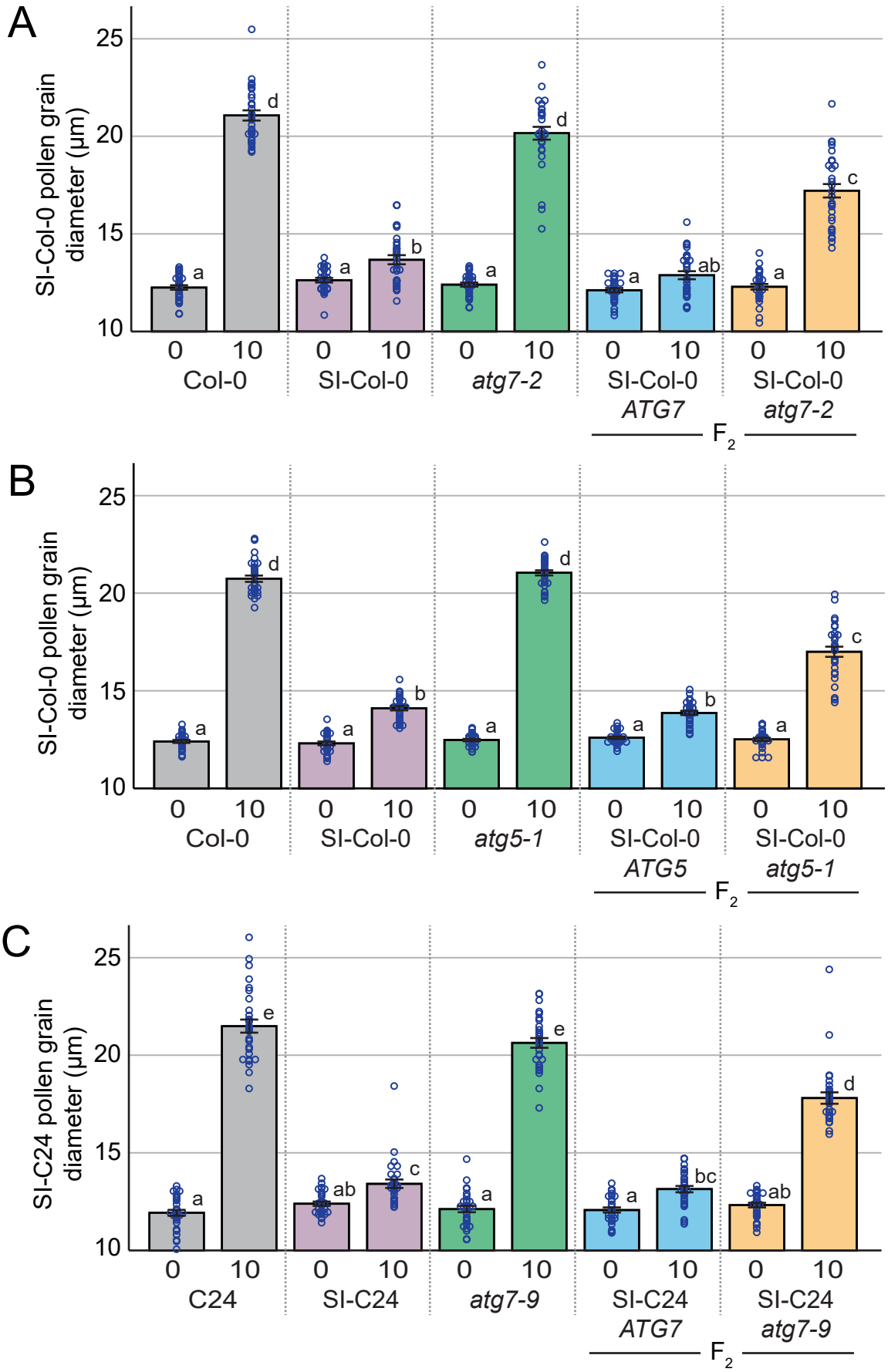

Figure 1. Pollen hydration assays on control and SI F2 progeny segregating for the *atg7* and *atg5* mutations. Pollen hydration assays for **A,** SI-Col-0 pollen grains placed on stigmas from Col-0, SI-Col-0, *atg7-2*, and F2 progeny from the SI-Col-0 x *atg7-2* cross; **B,** SI-Col-0 pollen grains placed on stigmas from Col-0, SI-Col-0, *atg5-1*, and F2 progeny from the SI-Col-0 x *atg5-1* cross; and **C,** SI-C24 pollen grains placed on stigmas from C24, SI-C24, *atg7-9*, and F2 progeny stigmas from the SI-C24 x *atg7-9* cross.
Pollen hydration was measured by taking pollen grain diameters at 0- and 10-minutes post-pollination. Data is shown as Mean +/- SE with all data points displayed. n=30 pollen grains per line, P<0.05 (One-way ANOVA with Tukey-HSD post-hoc test).

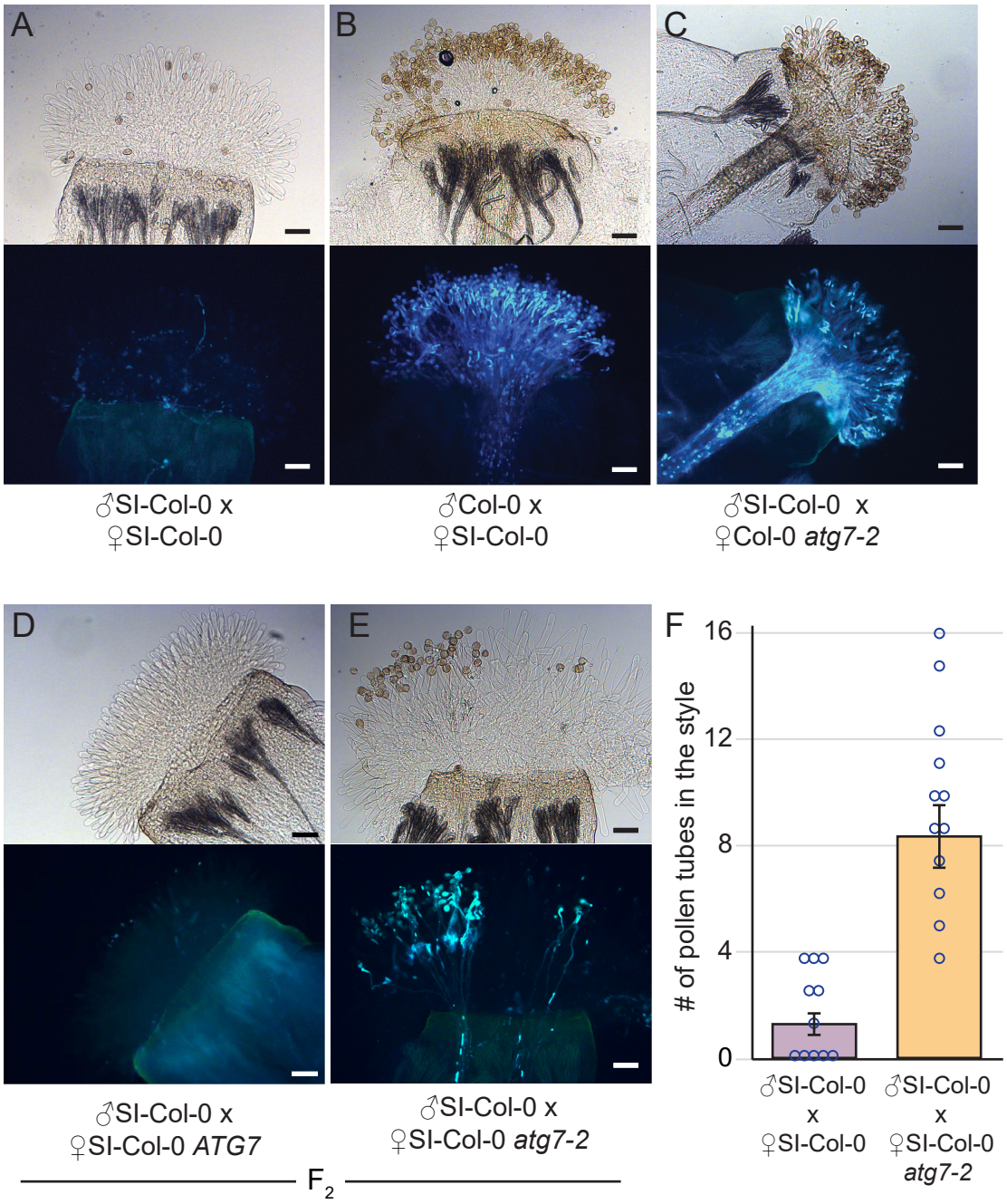

Figure 2. Representative images of aniline blue-stained SI-Col-0 or SI-Col-0 *atg7-2* pistils at 24 hrs following pollination.

A-E, All stigmas were hand-pollinated with SI-Col-0 pollen or wild-type Col-0 pollen as indicated and collected at 24 hours post-pollination for aniline blue staining. The genotypes of the pistils are indicated for each panel. Pollen tubes penetrating through the stigma and style indicate a breakdown of self-incompatibility as seen in E. For each panel, top image = brightfield, bottom image = aniline blue. Scale bar = 100µm

F, Bar graph showing the mean number of pollen tubes at 24 hrs post-pollination. Data is shown as Mean +/- SE with all data points displayed. n = 11-12 pistils per line. At 24 hours, pistils from SI-Col-0 *atg7-2* mutants allowed a significantly higher number of SI-Col-0 pollen tubes compared to the SI-Col-0 pistils ($P<0.05$).

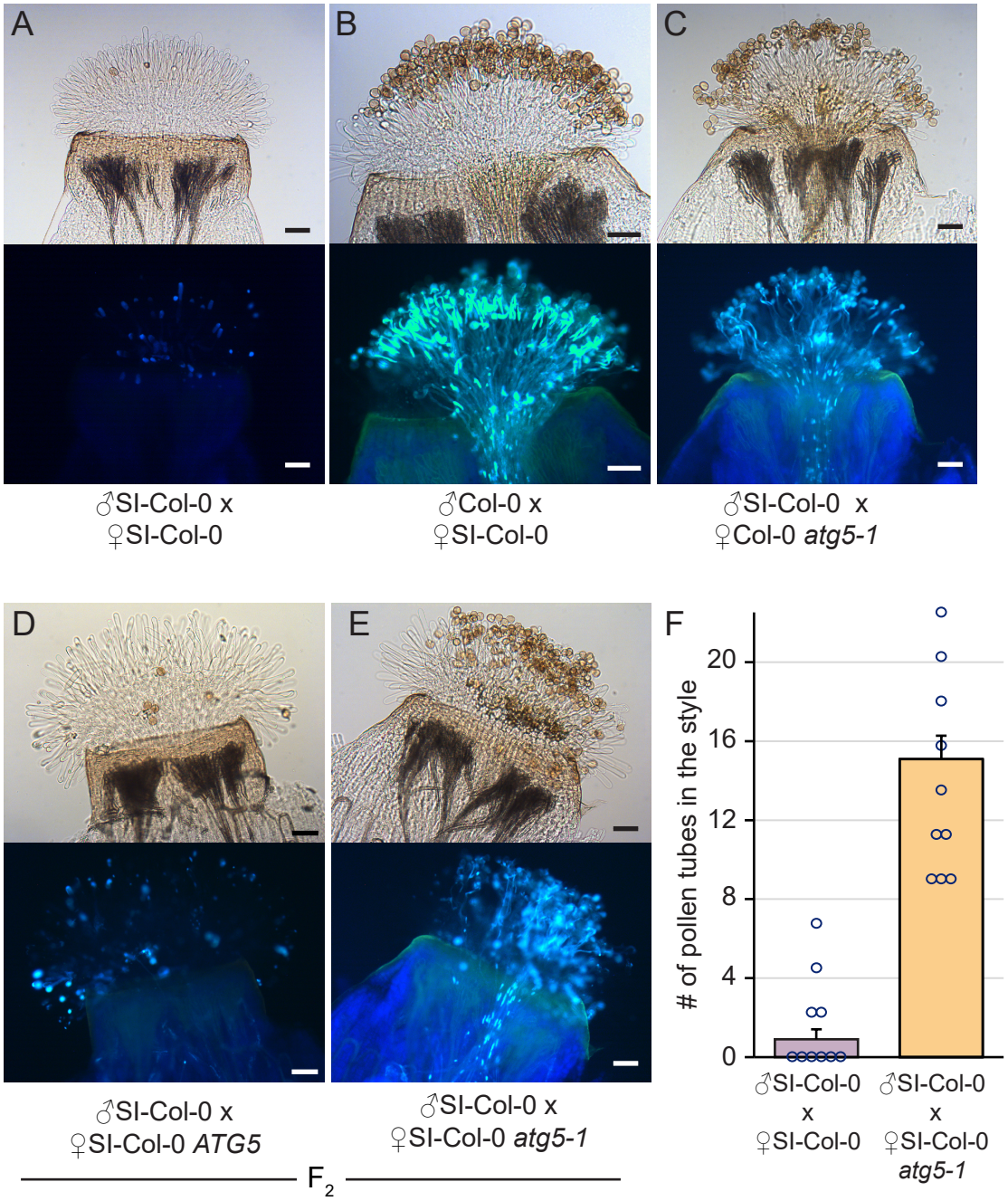

Figure 3. Representative images of aniline blue-stained SI-Col-0 or SI-Col-0 *atg5-1* pistils at 24 hrs following pollination.

A-E, All stigmas were hand-pollinated with SI-Col-0 pollen or wild-type Col-0 pollen as indicated and collected at 24 hours post-pollination for aniline blue staining. The genotypes of the pistils are indicated for each panel. Pollen tubes penetrating through the stigma and style indicate a breakdown of self-incompatibility as seen in E. For each panel, top image = brightfield, bottom image = aniline blue. Scale bar = 100μm

F, Bar graph showing the mean number of pollen tubes at 24 hrs post-pollination. Data is shown as Mean +/- SE with all data points displayed. n = 10 pistils per line. At 24 hours, pistils from SI-Col-0 *atg5-1* mutants allowed a significantly higher number of SI-Col-0 pollen tubes compared to the SI-Col-0 pistils ($P<0.05$).

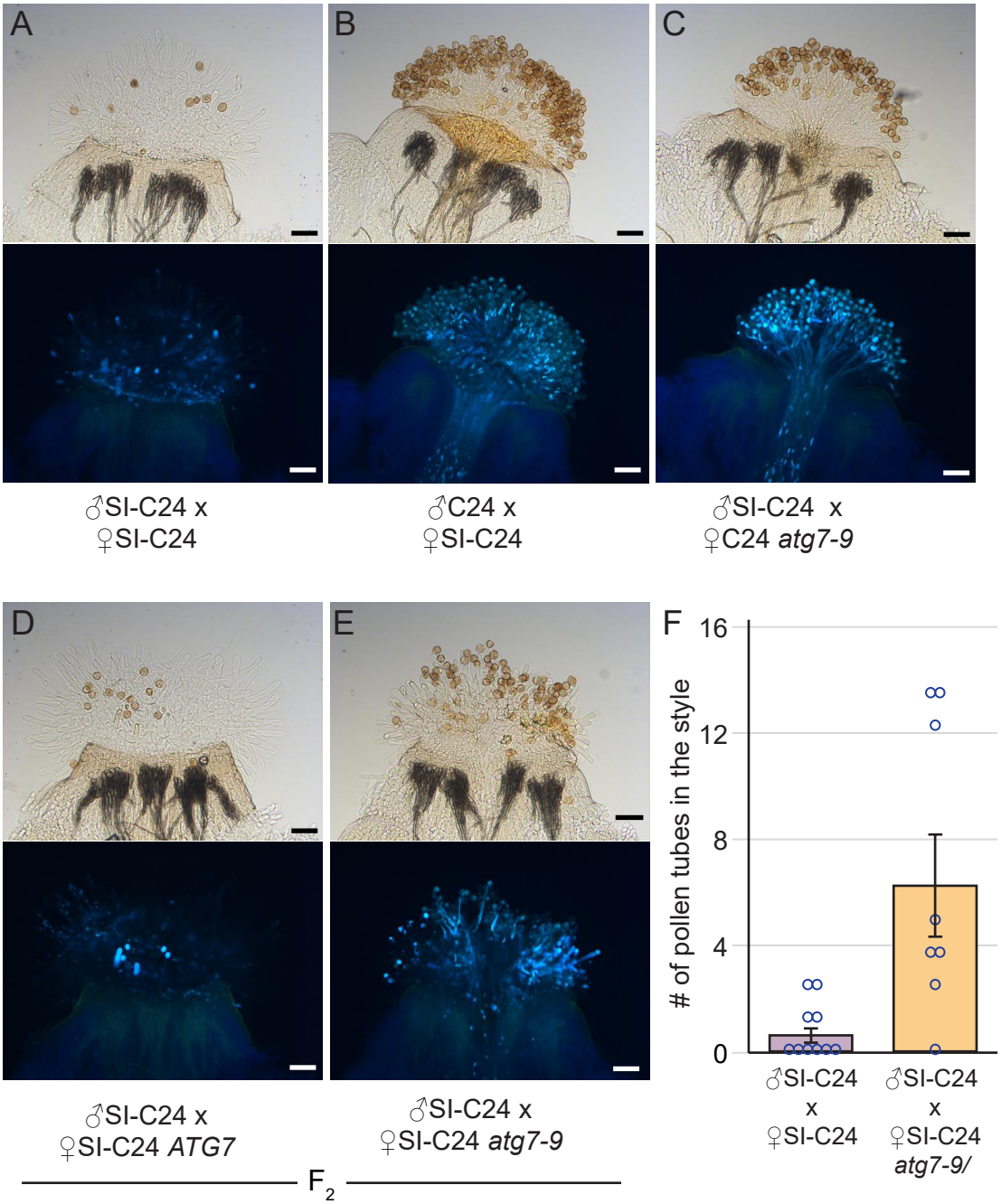

Figure 4. Representative images of aniline blue-stained SI-C24 or SI-C24 *atg7-9* pistils at 24 hrs following pollination.

A-E, All stigmas were hand-pollinated with SI-C24 pollen or wild-type C24 pollen as indicated and collected at 24 hours post-pollination for aniline blue staining. The genotypes of the pistils are indicated for each panel. Pollen tubes penetrating through the stigma and style indicate a breakdown of self-incompatibility as seen in E. For each panel, top image = brightfield, bottom image = aniline blue. Scale bar = 100µm

F, Bar graph showing the mean number of pollen tubes at 24 hrs post-pollination. Data is shown as Mean +/- SE with all data points displayed. n = 8-10 pistils per line. At 24 hours, pistils from SI-C24 *atg7-9* mutants allowed a significantly higher number of SI-C24 pollen tubes compared to the SI-C24 pistils ($P<0.05$).

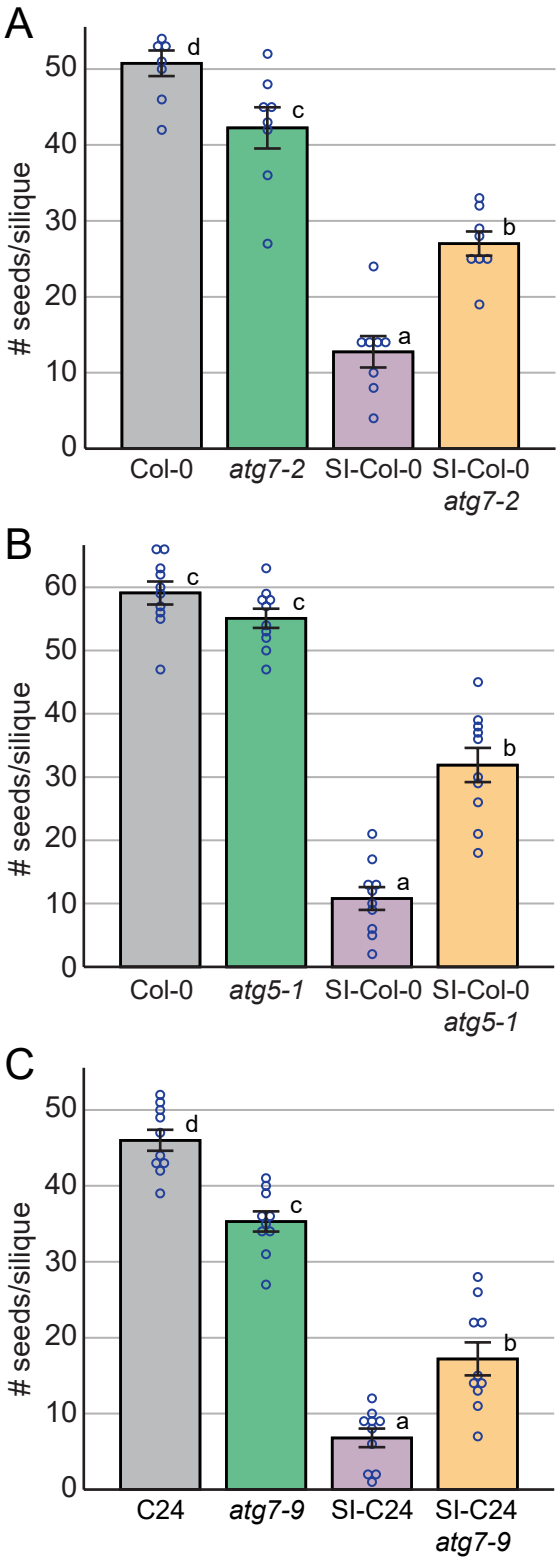

Figure 5. Seeds per silique counts for control and SI plants with the *atg7 or atg5* mutations. Seeds per silique counts following manual pollination with **A, B,** SI-Col-0 pollen or **C,** SI-C24 pollen on pistils with the indicated genotypes. Siliques were harvested at 2-weeks post-pollination and cleared for seeds counts. Data is shown as Mean +/- SE with all data points displayed. n= 8-10 siliques per line. Compared to the control SI pollinations, significant increases in the number of seeds per silique were observed for the SI plants that were homozygous for the *atg7* or *atg5* mutations, $P<0.05$ (One-way ANOVA with Tukey-HSD post-hoc test).

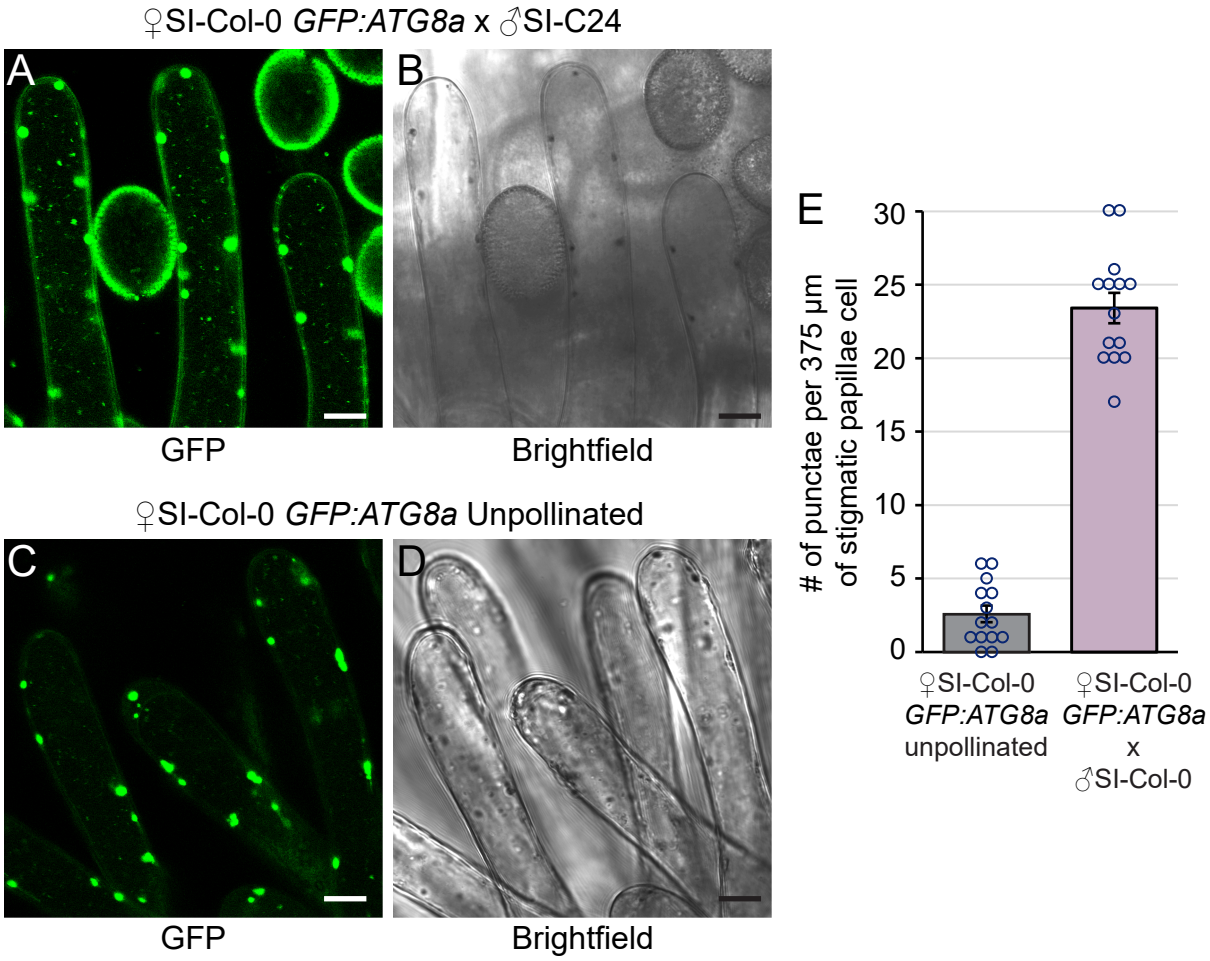

Figure 6. Autophagosomes are more abundant in SI-Col-0 *GFP-ATG8a* papillae following pollination with SI-Col-0 pollen

More autophagosomes marked by GFP-ATG8a are visible at 15-minutes post-pollination in the SI-Col-0 *GFP-ATG8a* papillae (**A-B**) compared to unpollinated SI-Col-0 *GFP-ATG8a* papillae (**C-D**). Scale bar = 10µm.

E, Bar graph showing the mean number of autophagosomes present in each sample. Data is shown as Mean +/- SE with all data points displayed. n=14 papillae. At 15 min post-pollination with SI-Col-0 pollen, there is a significant increase in the number of GFP-labelled punctae in the SI-Col-0 GFP-ATG8a papillae ($P<0.05$). The large punctae are chloroplasts with autofluorescence and were not counted.